I&EC research
Industrial & Engineering Chemistry Research

Article

Modeling Pore-scale Two-phase Flow: on How to Avoid Gas Channeling Phenomena in Micropacked-Bed Reactors via Catalyst Wettability Modification

Francisco José Navarro-Brull, and Roberto Gómez

Ind. Eng. Chem. Res., **Just Accepted Manuscript** • DOI: 10.1021/acs.iecr.7b02493 • Publication Date (Web): 29 Nov 2017

ACS Publications

Industrial & Engineering Chemistry Research is published by the American Chemical Society. 1155 Sixteenth Street N.W., Washington, DC 20036

Modeling Pore-scale Two-phase Flow: on How to Avoid Gas Channeling Phenomena in Micropacked-Bed Reactors via Catalyst Wettability Modification

*Francisco J. Navarro-Brull, Roberto Gómez**

Institut Universitari d'Electroquímica i Departament de Química Física, Universitat d'Alacant, Apartat 99, E-03080, Alicante, Spain

ABSTRACT. A model for the design of micropacked-bed reactors via correlations, capable of providing a reliable estimation of two-phase flow dynamics and mass-transfer coefficients, is lacking, especially when the particle size of the bed is around 100 μm. In this work, we present a validation of the use of the phase-field method for reproducing two-phase flow experiments found in the literature. This numerical simulation strategy sheds light on the impact of the micropacked-bed geometry and wettability on the formation of preferential gas channels. Counter-intuitively, to homogenize the two-phase flow hydrodynamics and reduce radial mass-transfer limitations, solvent wettability of the support needs to be restricted –showing best performance when the contact angle ranges 60º and capillary forces are still dominant. The tuning of gas-liquid-solid interactions by surface wettability modification opens a new window of opportunity for the design and scale-up of micropacked-bed reactors.

KEYWORDS: phase field method, micropacked bed, gas channeling, capillary fingering, wettability, contact angle

Introduction

Process intensification has been one of the most promising areas of study since it can enable novel reaction methods by scaling down the dimensions of chemical reactors. Packed-bed microreactors are well known because of the versatility for testing catalysts since they allow to quantitatively measure kinetics, performance, and deactivation.[1–5] However, kinetic and transport phenomena rely on the complex hydrodynamic characteristics of these systems.[6] Among their advantages, these miniaturized packed bed reactors have unique heat- and mass-transfer characteristics thanks to high surface-to-volume ratios that the miniaturization of the reaction channel and catalyst particles provides. Yet, this reduction of diameter and particle size entails a substantial pressure drop that is difficult to overcome since a numbering-up strategy —i.e. adding multiple reactor channels— will tend to cause flow maldistribution. Another option is to scale microreactors up to the range of milli-reactors (with reactor inner diameters in the order of tens of mm).[6] In both cases, when the catalyst particles are smaller than ~500 μm, the hydrodynamics are usually dominated by viscous stress and interfacial tension at the liquid-gas boundary rather than by gravity and inertial forces.[7,8] Larger scale packed-bed reactors in which the catalyst pellets are about 1-3 mm —generally known as trickle-bed reactors— have semi-empirical equations that are commonly used for design purposes.[9] However, the inherent packing randomness combined with the strong capillary and viscous forces in micropacked-bed reactors preclude the use of simple and accurate modeling equations to predict mass-transfer coefficients under different conditions.

In the literature, several authors have applied visualization techniques to gain a physical understanding of micropacked-bed media. The usual approach is to use micro-fabricated plate-beds.[10–14] For example, Marquez built a series of microdevices with micropillars to have a clear 2D visualization of the complex hydrodynamics at these scales.[10] These authors showed that, even when using an ordered array of micropillars of 120 μm in diameter each, preferential channels of gas (i.e. gas channeling) were present. The different flow patterns obtained highlighted how some critical parameters —fluid viscosity ratio, surface tension, and geometry including its wettability— determine the hydrodynamics of these miniaturized systems. Similarly, the use of small catalyst particles —i.e. <500 μm of diameter approximately— in miniaturized packed-bed reactors present the following characteristic behavior (Figure 1):[15]

- bed is usually saturated with liquid due to strong capillary forces;
- gas exclusively flows through the packed-bed along preferential channels;
- pre-wetting of the system or modification of flow rates do not significantly affect the path once the flow is stabilized.

As a result of the preferential channels, poor radial dispersion and conversion are generally obtained.[16,17] In contrast to the larger trickle-bed reactor scale, capillary forces strongly depend on particle size distribution, shape, and wettability of the catalyst. Thus, due to the inherent randomness of the packing and particle properties, it is possible to anticipate a lack of general reproducibility when carrying out reactions in these miniaturized systems. More importantly, a poor radial dispersion is obtained when preferential paths for the gas phase —not for the liquid phase as it happens for trickle-bed flows— appear. The change of the fluid dynamic behavior when reducing the particle size, modifies the nature of preferential flow paths or "channels" being formed (see Figure 1). In this way, modeling strategies for trickle-bed reactors, which have

been based on empirical hypotheses, cannot be extended to miniaturized devices dominated by viscous stresses and interfacial tension forces.[18]

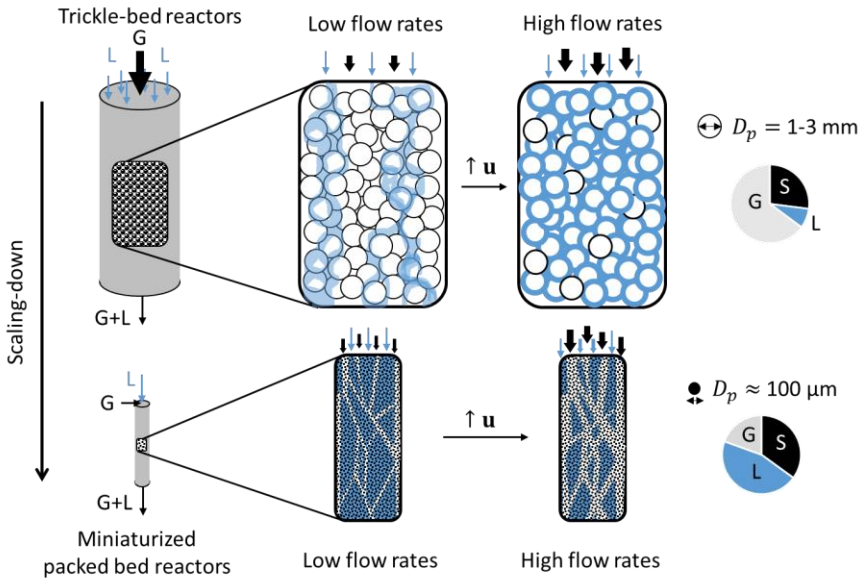

Figure 1. Conceptualized representation of the hydrodynamic behavior for a macro-scale packed-bed reactor or trickle-bed reactor (top) and a miniaturized packed-bed reactor (bottom). The pie chart shows the volumetric fraction of solid, liquid and gas in the bed (reciprocal of porosity, liquid and gas hold-up, respectively). Adapted with permission from ref. 15. Copyright (2010) American Chemical Society

Larachi et al. studied the influence of the bed geometry and particle size via wall microscopic visualization and residence time distribution (RTD).[19,20] Wetting patterns and transient times (i.e. time required to achieve a steady state) were significantly affected when changing the particle size diameter from ~53-63 µm to 106-125 µm, whereas a change of the bed cross section geometry (circular or square) did not have a significant effect. This study helped visualize gas-

liquid interaction right downstream gas and liquid reactor inlets and to understand how reduced particle sizes achieved earlier the high gas-liquid interaction regime (desired on this scale). In fact, mass transfer coefficients of miniaturized packed-beds are intimately linked to gas-liquid interactions —where channeling phenomena are to be avoided—.[21,22] If one tries to reduce the high pressure drop by increasing the reactor diameter, the mass-transfer coefficients are significantly reduced due to these preferential paths being formed. Moreover, the confinement of particles near the wall introduces structural irregularities that cannot be avoided. This increase of porosity near the wall promotes the appearance of another type of preferential channel known as wall channeling. In order to deal with these effects from the modeling point of view, one can use theoretical mass transfer coefficients with penalization factors that account for the radial dispersion and partial wettability.[17]

Albeit flow regime maps can be depicted for each application, there is still a plethora of parameters —i.e. liquid and gas velocities, the physical properties of the fluids, characteristics of the solid surfaces, inherent construction errors or even the design of the fluid inlets— that cannot be taken into account in simple models.[16] For instance, the combined effect of capillary forces, viscous forces and wettability (impact of the contact angle) has not been elucidated until very recently with the aid of Hele-Shaw cell geometries.[23–25] These studies are part of numerous efforts to understand multiphase flows through porous media similar to microparticulate packed-beds in other areas of research: oil recovery[26,27] and geological carbon dioxide sequestration,[28,29] among others.[30] Interestingly, all these works show improvements when the wettability of the displacing fluid is restricted up to a certain value of contact angle.[31] In liquid-liquid porous application domains, preferential channels are usually classified as either capillary or viscous fingering.[32] The capillary number ($\mathrm{Ca} \cong \mu u/\gamma$) is used to discern which kind of fingering may

occur, where γ is the surface tension, μ the viscosity and u the velocity of the fluid being displaced. Interestingly, for capillary flow regimes ($Ca \ll 1$), reducing the surface wettability of the particles can help to reduce flow maldistribution to some extent.[24,33,34]

To understand the formation of preferential channels in micropacked-bed reactors (also known as miniaturized packed-beds), a computational model is proposed in this work. First, a literature case is used to validate the selected modeling approach (Phase Field Method, PFM) under different conditions. Later, we identify key parameters that can significantly reduce gas-channeling problems such as packed-bed geometry and wettability. Our findings can be primarily used for the design of new catalysts/beds that improve the hydrodynamics in random micropacked beds at different scales, ultimately reducing several of the existing mass-transfer unknowns and limitations.

Theory and numerical methods

Two main approaches haven been proposed to address the question of simulating two-phase flows at the particle- or pore-scale: interface tracking and interface capturing.[35] To simulate the bubble breakup and coalescence through a porous medium, two popular interface capturing approaches are the level set (LSM) and the PFM.[35,36] Usually, PFM is preferred over LSM since it is a physically-based method and provides more accurate and efficient results.[36,37] In addition, PFM can be successfully coupled with heat transfer equations[38] at this simulation scale. Another strategy to model the two-phase flow commonly used is the Volume of Fluid Method (VoF).[39–42] However, the VoF method cannot capture the curvature of the interface properly, leading to spurious or parasitic velocities that need a special treatment[37,43]. Very recently, meshless methods, such as the Smoothed Particle Hydrodynamics (SPH) method have been also used and

validated for porous structures.[44] Another interesting modeling approach is to combine multiple lengths and timescales, only focusing on the interface while solving Darcy (porous) formulations in saturated domains.[45–49]

The main practical advantage of using the PFM is the minimum parameter tuning required to obtain accurate results[36,37] and the ability to combine it with other physics of interest.[38] Thus, in this work, we have used the finite-element method (FEM) to solve the PFM equations via the commercial software COMSOL Multiphysics™. Although a comprehensive explanation of the PFM formulae is given in the Supporting Information, a detailed description of the numerical schemes —necessary to solve this system with a fourth-order partial differential equation— can be found in the literature.[36,38,49]

Literature case review and model validation

Micro-fabricated bed for two-phase flow studies

Marquez carried out gas-liquid flow visualization studies through a micro-fabricated plate with different pillar array geometries[10]. Ethanol and polyethylene glycol 200 (PEG-200) were fed to the constructed micro-fluidic device made of polydimethylsiloxane (PDMS). The authors performed several experiments introducing one of these two liquids and air to modify the viscosity ratios and interfacial tension forces while maintaining the system geometry. In this way, they studied hydrodynamic interactions to identify relevant parameters while gaining a physical understanding of the flow pattern in packed-bed microreactors. Concretely, authors used a uniform packed ⌀ 120 μm micro-pillar configuration (A^*_2 lattice) with a center-to-center distance of 150 μm. More details of the micro-fabricated device can be found in 10.

The dimensions and hydrodynamic parameters used in this work are shown in **Table 1**. The reader should note that, to limit computational costs, the geometry was reduced to a representative elementary volume (REV). Thus, the micro-fabricated device[10] was not entirely modeled and, more specifically, the gas and liquid inlets and pillars were placed with the intention of minimizing their impact on the simulation results. Symmetry planes were used at the extremes of the domain. Albeit authors did not mention the quality of the construction, a zero-centered Gaussian distribution curve with a standard variation for the micro-pillar position of 5 μm was chosen. This random construction lumps together all the possible geometric and surface inhomogeneities that are inherent to the system. The visualization experiments[10] were performed within a few hours (short term experiments) in order to maintain constant the value of the contact angle. No mention is made to any type of dimensional change observed during the experiments. Actually, the same device was used with induced either hydrophilic or hydrophobic surfaces, without any noticeable charge in the device geometry.

Table 1. Liquid properties and dimensions of the domains for the simulations of micro-fabricated bed devices by Marquez et al.[10]

Simulation domain	**Liquid**	**width** [mm]	**height** [mm]	μ_L [mPa·s]	σ [mN·m^{-1}]	u_L [mm·s^{-1}]	u_G [mm·s^{-1}]	θ
1	ethanol	2.25	1.8	1	22	2.7	52.7	37.8º
2	ethanol	2.25	1.8	1	22	2.7	52.7	6º
3	PEG-200	2.25	1.3	37.7	44	6	50.3	45º

Different contact angles were used as boundary conditions (see **Table 1**). As the authors described,[10] they modified the wettability of the PDMS with a plasma treatment. For the system with PEG-200/air, the authors did not specify the value of the contact angle. Given the nature of both solvent and surface, and in order to avoid artificially added capillary effects, a constant value of 45° was chosen for the contact angle.

Computational resources are the limiting factor for two-phase flow simulations via PFM. At this simulation scale, it is not clear whether 3D models —which require the use of high-performance computers with hundreds or thousands of cores— are necessary in order to obtain more accurate results.[40] Thus, in agreement with other authors, we believe that the 2D-model presented here could be used to understand the effect of relevant parameters that tend to be disregarded during reactor design.

As this microfluidic device is very thin with rather low velocities (laminar flow), the real 3D system was modeled according to the PFM and laminar 2D formulation as described in the Supporting Information. Triangular meshing and reduced time-step sizes were controlled by COMSOL MULTIPHYSICS (v4.4 and 5.2, COMSOL AB) numerical solvers using a backward differentiation formula. As mentioned earlier, the refinement of the mesh was performed solely in the vicinity of the gas-liquid interface where a 5μm finite element size was used for the rest. This approach significantly reduces computational cost and allows to obtain simulation results on the time scale of a few days using a computer with two 12-core Intel Xeon E5 processor.

Hydrodynamic Model Validation of a Two-phase Flow

For the air/ethanol system, Figure 2 compares the results where the wettability was modified (contact angle of 37.8º and 6º, respectively). Since the provided images of the actual experiments were captured at a much slower speed than the physics of interest, we selected three situations

where the flow pattern differed. For the sake of visual comparison, similar color code is maintained both in experiment and simulation results.

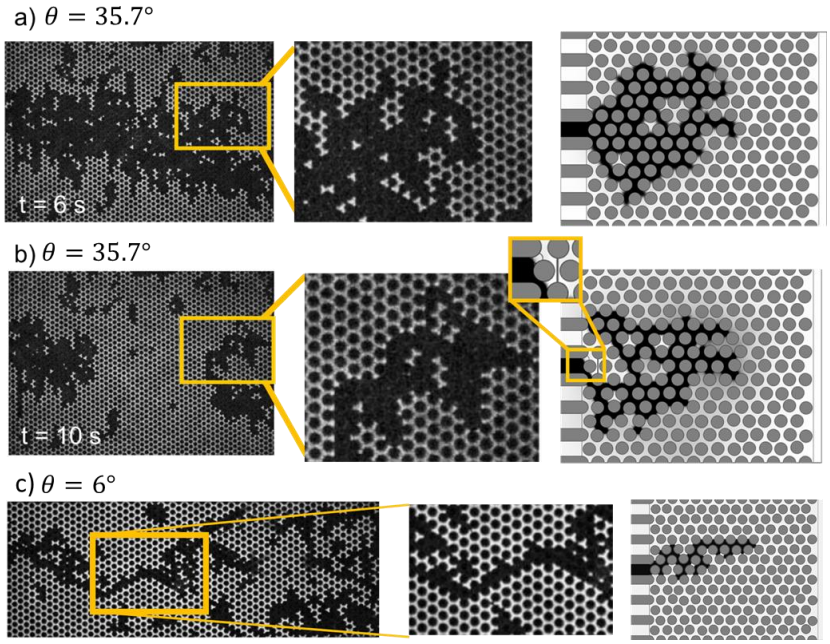

Figure 2. Comparison between flow patterns obtained in the experiments (left and center column) and via PFM-model simulation (right column) for the ethanol/air system. For the experiments, white/gray color represents the liquid, whereas black color indicates the gas phase and micro-pillar sections. For the simulation results (right column), gray color represents the micro-pillars instead. First row (a) has a direct feed of gas while second row (b) has an obstacle at the entrance to test inlet effects. The third column (c) corresponds to an increase in wettability of the liquid (change in contact angle from 35.7 down to 6º) manifesting gas channeling issues at these scales. Experimental results adapted with permission from ref. 10. (Copyright 2010) Marquez Luzardo, N. M.

In both cases, we can see that the simulated flow patterns reproduce liquid enclosures inside the gas bubbles as well as the fingering movement of the gas (Figure 2). The model geometry used in Figure 2b was slightly modified as well —note the obstacle represented by a thin wall between two pillars located in front of an inlet. This was done in order to assess the impact of a significant inlet modification on the simulated flow patterns obtained. As mentioned, the case of a PEG-200/air two-phase flow was also simulated. Figure 3 shows a comparison of two flow patterns.

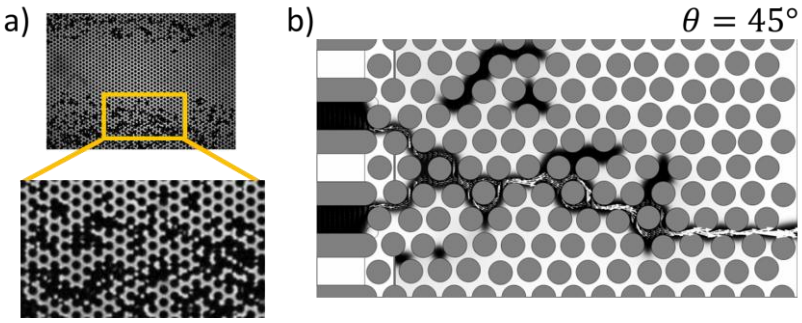

Figure 3. Comparison of flow patterns obtained from the experiments (a) and from the 2D-model (b) for the PEG-200/air system (Table 1, third row). For the experiments, white/gray color represents the liquid, whereas black color indicates gas phase and micro-pillars. For the simulation results, similar color code was chosen to ease the comparison. White arrows on the right indicate the velocity field showing a main preferential gas channel stream. Experimental results adapted with permission from ref. 10. (Copyright 2010) Marquez Luzardo, N. M.

Again, we can see that the model matches the experimental micro-scale results. Particularly, the increase of surface tension of the liquid shortens the gas slugs and reduces the size of the

bubbles. The placement of obstacles nearby the gas and liquid inlets create enough perturbation to obtain characteristic flow paths within the reduced simulation domain.

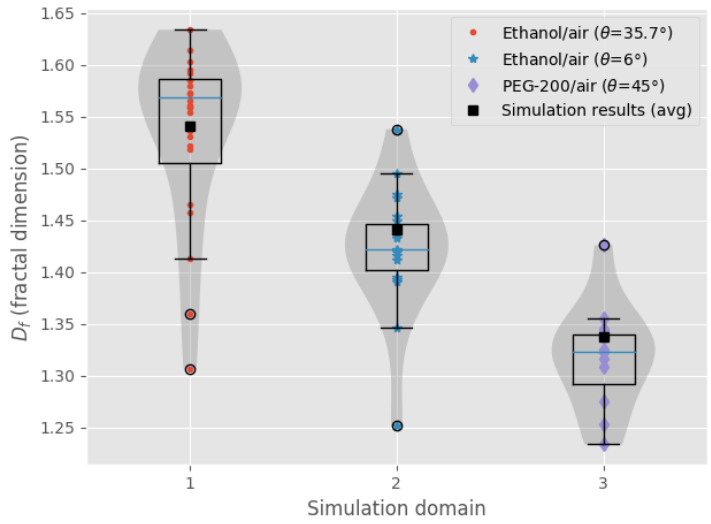

Figure 4. Self-similarity of the studied gas flow patterns. For the experimental results, colored points represent each of the subsampled fractal dimension obtained. The statistical distribution of the experimental results is also shown via embedded boxplot and violin plots. Within the interquartile range, square dots represent the averaged fractal dimension of simulation results.

To quantify the statistical self-similarity between the flow patterns, the fractal dimension was computed by subsampling the experimental and simulation results (see SI). Despite the complexity of the transient flow under study, the fractal dimension of the simulated gas-flow patterns are contained within the interquartile range of the experimental data set (Figure 4). The expected differences are attributed to the inlet configuration and inhomogeneous geometry and material wettability,[40] which are common uncertainties found experimentally.[10] This agreement

points to the fact that PFM is a powerful tool able to capture and foresee the fundamental physical characteristics of the two-phase flow on the scale of the micropacked bed.

Discussion: predicting and reducing gas channeling

Once we validated the model, flow patterns as a function of some physical parameters can be further investigated. Concretely, the effect of gas and liquid flow rates as well as the contact angle is discussed for a micropacked-bed geometry intended for carrying out hydrogenation reactions.

Packed-bed geometry and flow rate impact

Two-phase flow CFD results have shown a strong dependence on the geometry being simulated, especially with particle diameters below 500 μm, where the hydrodynamics are dominated by viscous stress and interfacial tension forces. We have used two model systems to illustrate gas-channeling phenomena:

1. A random 2D geometry that maintains void distances among variable diameter particles, mimicking a real porous skeleton.
2. A 2D section from a 3D random arrangement computationally generated using a Monte Carlo approach.[50,51]

In dealing with the first system, we can define now our REV as a rectangular domain of 1 mm in height and 0.5 mm in width, including a random distribution of particle diameters mean-centered at 100 μm (Figure 5). Analogous boundary conditions to those described earlier were used. Thus, the following models will evaluate the evolution of a preferential gas channel through a micropacked-bed not affected by the reactor walls. To demonstrate the effect of

extreme case scenarios, volumetric flow rates of both fluids are ranging from 1 to 15 mL·min^{-1} for the liquid and from 50 up to 200 mL·min^{-1} for the gas —through a packed-bed of 10 mm of inner diameter— (see

Table **2**). As for the rest of fluid dynamics parameters, between the solvent and the gas (hydrogen), the interfacial tension is 20 mN·m^{-1} whereas the log of density and viscosity ratio are 4 and 3, respectively. For these simulations, a constant contact angle of 45º for the wetting phase was considered.

Table 2. Flow rates and superficial velocities applied for the analysis of gas channeling in a 2D packed bed geometry

Simulation	**a**	**b**	**c**	**d**
$\boldsymbol{F_L}$ [mL·min^{-1}]	10	10	1	15
$\boldsymbol{F_G}$ [mL·min^{-1}]	50	200	100	100
$\boldsymbol{u_L}$ [mm·s^{-1}]	2.1	2.1	0.2	3.1
$\boldsymbol{u_G}$ [mm·s^{-1}]	10.6	42.4	21.2	21.2

From the simulation results shown in Figure 5 (a, b, c, d and e), it can be seen how the main preferential gas channels and liquid hold-up did not differ significantly for different flow rate ratios. A reactant tracer was introduced with the gas to give an intuition of the residence time differences among the different cases.

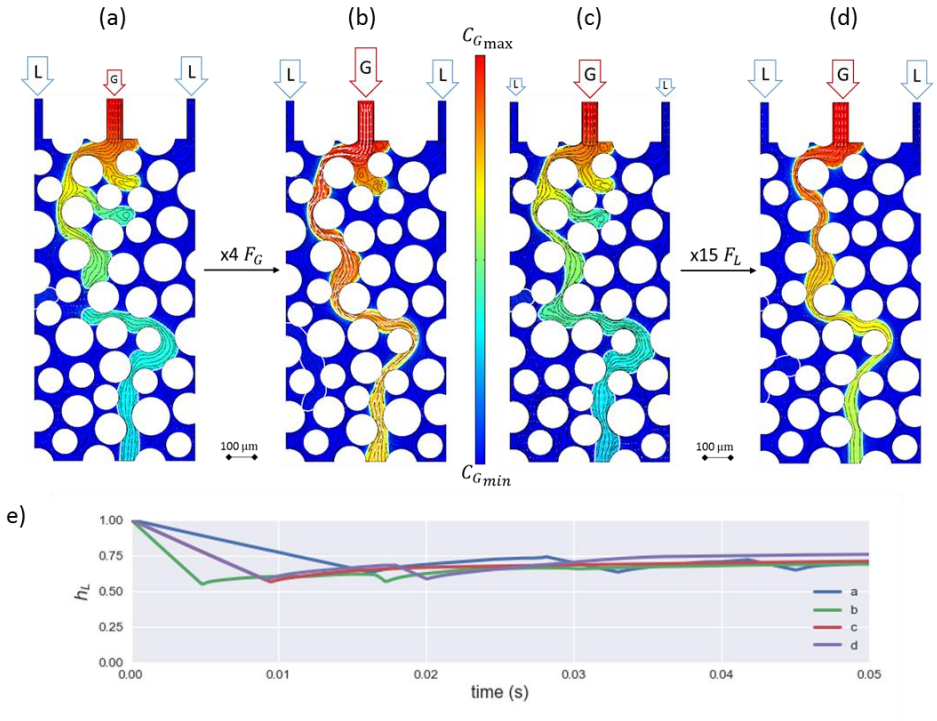

Figure 5. Array of particles simulating a miniaturized packed-bed showing gas channeling at different flow rates after flow stabilization. Color indicates the concentration of a reactant tracer in the gas. Even increasing four times the gas flow rate (from a to b) or the liquid flow rate by a factor of 15 (from c to d), long term flow paths show almost identical gas channeling behavior. A plot of liquid hold-up as a function of time is given in (e).

These results illustrate one of the main limitations of packed-bed microreactors. In contrast to the behavior observed in trickle-bed reactors —where the liquid, and not the gas, forms preferential channels—, wettability issues cannot be generally solved by increasing flow rates. Gas-channeling is mainly dependent on the (random) pore structure. This allows to gradually grasp the difficulty of obtaining simple correlations to predict design parameters.

Influence of the Contact Angle

To the best of our knowledge, the effect of the contact angle in packed-bed microreactors has not been thoroughly studied yet. However, very recently it was found that a partially wet bed led to the best yields in a packed-bed microreactor, outperforming batch results.[52] However, this flow pattern was obtained as an optimal combination of gas and liquid flow rates rather than through surface wettability control. There is a growing interest in the effect of contact angle —including advanced modeling considerations— in capillary systems similar to packed-beds.[25,27,53,54]

As seen in the validation results (Figure 2a and b compared to c), varying the contact angle has a significant impact on gas channeling. Fluid-fluid wettability control has been recently demonstrated in Hele-Shaw packed cells for capillary flow regimes.[24,33] We can further visualize this effect using the geometry defined in Figure 5 as well as boundary conditions for the case described in Table 2b (unfavorable conditions to see channeling effects). Gas preferential paths for three different contact angles are shown (Figure 6) after 10 ms. The use of constant or static values of contact angle is an adequate modeling assumption with this working geometry and scale.[55]

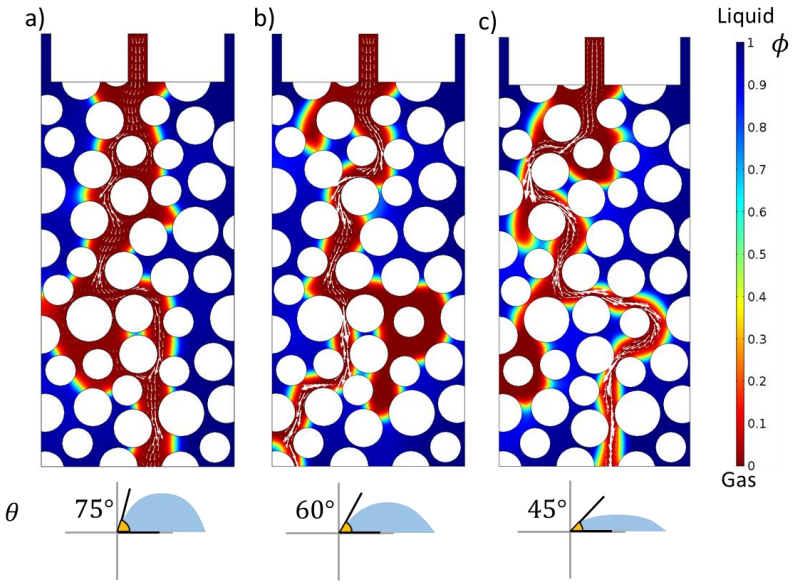

Figure 6. Simulation results of an organic solvent (l) and H_2 (g) through a REV domain of a randomly packed columns of 100 μm in diameter (mean-centered). Results are calculated for (a) 75, (b) 60 and (c) 45° contact angle values leading to an increase of gas channeling. The gas phase is represented in red and the liquid in blue. Green colors correspond to the gas-liquid interface, while small white arrows indicate the velocity field.

Marquez also documented this particular behavior with the ethanol/air flow system. Authors mentioned explicitly how contact angle produced a significant impact on the flow pattern increasing the "snaking" movement of the bubbles being formed[10]. In this regard, both simulation and experimental results confirm the wettability impact when working at miniaturized scales in packed-bed reactors. Thus, the question that arises now is whether there is an optimum contact angle that keeps high liquid hold-up values but reduces gas channeling (i.e. higher conversion and selectivity). We can perform a contact angle study in a 2D domain obtained from a section of a realistic 3D packing (second method described above) and statistically analyze gas-channeling

as a function of the contact angle for a scaled-up reactor at high superficial velocity speeds (0.1 $m \cdot s^{-1}$ and 0.05 $m \cdot s^{-1}$ for the gas and liquid, respectively). The velocity for the gas only doubles that for the liquid. This is consistent with reactions in which the substrate that reacts with the gas is dissolved in an appropriate solvent in such a way that its concentration has the same order of magnitude as the dissolved reactant.

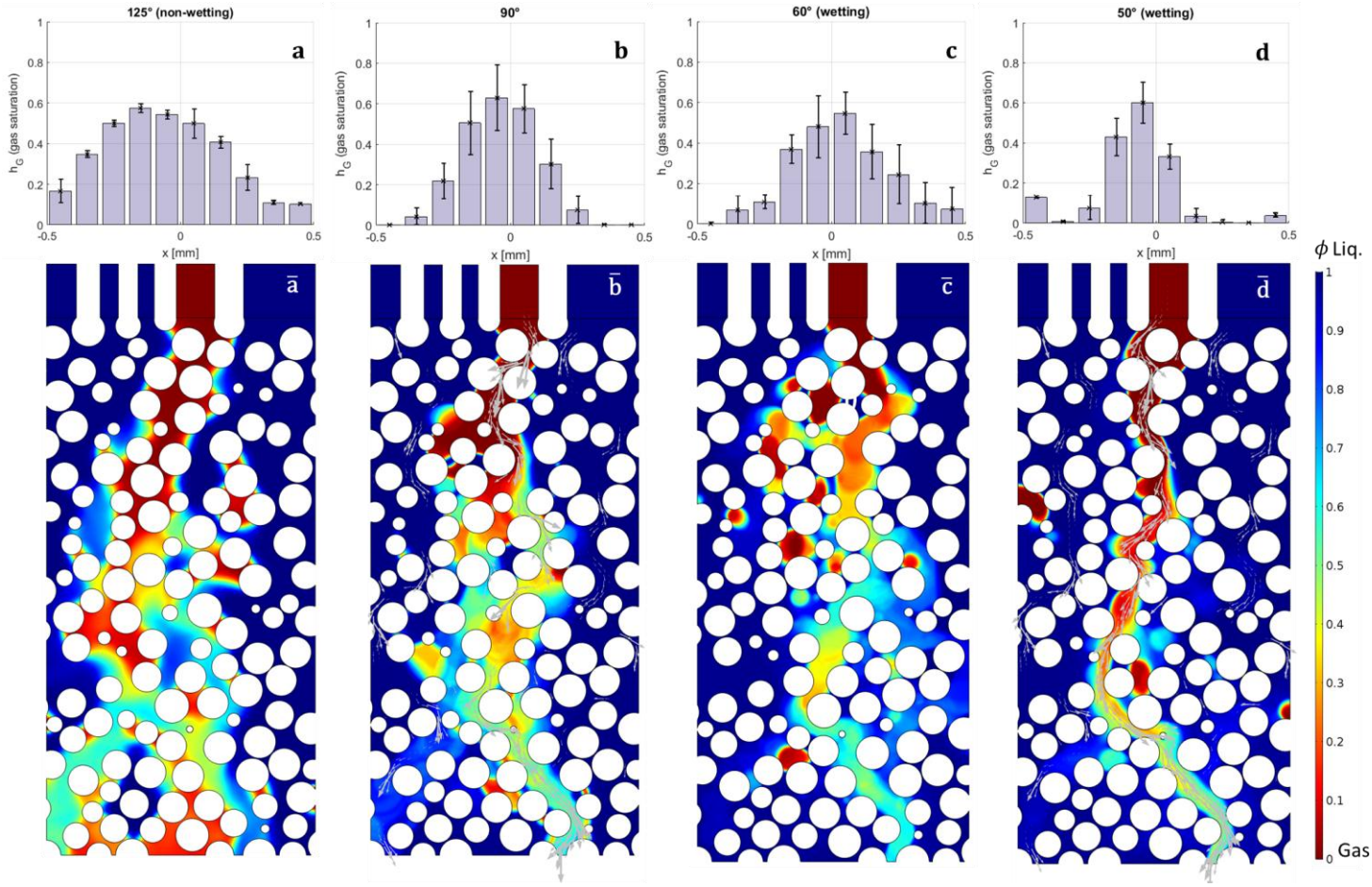

Figure 7. Histograms showing statistical results (time-average and standard deviation) of gas hold-ups (a, b, c, and d) as a function of contact angle. Below each histogram, a long exposure (time-averaged) pseudo-stationary saturation image (colored) of a 2D section packed-bed microreactor geometry with particles with of a mean-centered diameter at 100 μm ($\bar{a}$, $\bar{b}$, $\bar{c}$, and $\bar{d}$).

From the results shown in Figure 7, we can observe how increasing the wettability of the catalyst support produces more gas channeling. Instead of using a static image, a time average of the flow paths is computed, as if a long exposure image was taken, to better illustrate the gas channeling once the flow has been pseudo-stabilized. Specifically, the images in Figure 7 show surface maps of the local time-average values of the order parameter ϕ. The change of wettability can be quantified by comparing histograms that measure the gas volume fraction longitudinally. Note how, while maintaining similar absolute values, the distribution sharpens below 60º indicating the formation of preferential paths (Figure 7d compared to 6b and c). This does not seem an intuitive result. It is usually accepted that the catalyst support and solvent should be chosen to properly wet the catalyst surface since is at the solid-liquid interface where the hydrogenation reaction takes place. However, when radial-mass transfer problems appear due to gas channeling phenomena, the affinity of the liquid to the surface of the substrate needs to be diminished at least down to 60º. If the surface affinity to the liquid is misguidedly increased, channeling (Figure 7d) starts to occur. Note that at contact angle values of 40 or 30º (Figure 8), capillary forces start to produce bubble entrapments that are well captured by the dispersion that appears at the histogram (Figure 8b). If, in contrast, the surface is chosen to behave as non-wetting (above 90º as seen in Figure 7ā), the gas phase starts displacing most of the liquid, resulting into a wider distribution with minimal deviation (Figure 7a),

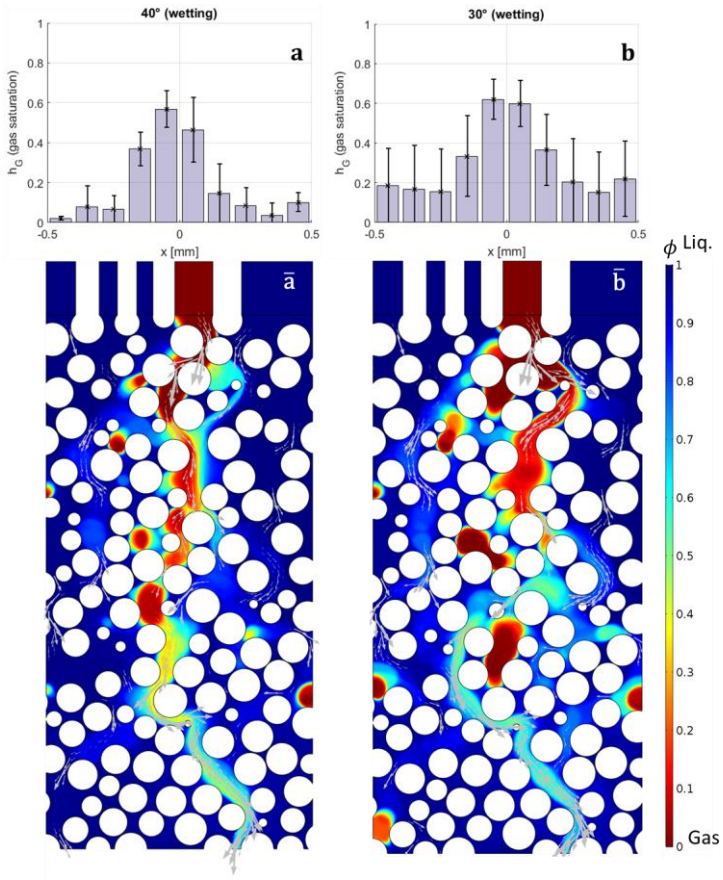

Figure 8. Histograms (a and b) show the quantitative results of the gas hold-ups (and standard deviation) for two values of the contact angle. The time-averaged pseudo-stationary saturation ($\bar{a}$ and $\bar{b}$, colored) illustrates how the confinement of bubbles occurs within the porous skeleton as the surface wettability increases. The 2D micropacked-bed geometry was generated from a 3D packing with a distribution of particle diameters mean-centered at 100 μm.

It is worth discussing further this significant hydrodynamic change for a contact angle of 60º. Let us first revisit recently published work in other areas where authors thoroughly explored, and rationalized channeling in porous media as a function of the contact angle either in experimental setups[24,33] or with new theoretical models.[25,53] Specifically, Trojer et al. stabilized the two-phase

flow fingering by modifying the surface wettability of Hele-Shaw packed cells with glass beads within capillary flow regimes.[33] Similar findings have been uncovered in geological CO_2 sequestration[28,29] or oil recovery[26,56] systems. On all the cited experimental works, there is one common pattern: capillary fingering is significantly reduced when the wettability is restricted (above 60º for the wetting phase).

The existence of a critical value of the contact angle around 60º during fluid invasion can be explained by the geometrical arrangement of the packed bed[57]. Irregular capillary forces are produced by the pore differences that appear among the different packing densities. When the particle arrangement nearly forms a regular lattice (either hexagonal or cubic close-packing), spheres tend to adopt tetrahedral pore structures where their centers form an angle of ~60º (see Figure 9). Under this close-packed arrangement, critical contact angle has been theoretically shown to appear when wettability is reduced above the 60-75º region,[31] increasing the probability of violent injections of fluid invading the porous structure (also known as Haines jumps). In this way, the physically-based PFM is not only able to reproduce experimental results, but also support these recent findings in other areas of research.

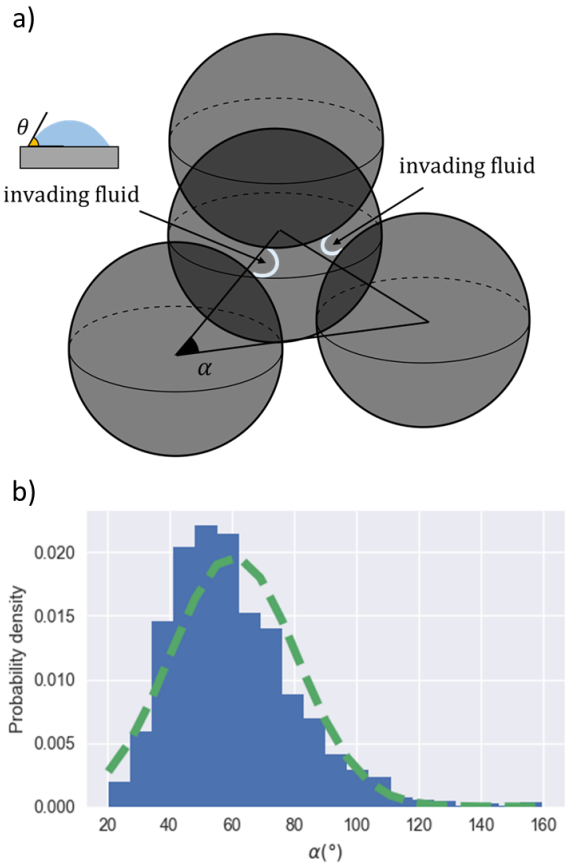

Figure 9. Sketch of a porous invasion mechanism[31] in a dense arrangement of randomly packed spheres (a), where θ indicates the contact angle of the displaced phase. Histogram (b) of the neighboring particle angle α for the 2D section of a closely-packed 3D geometry used in this work.

Similar trends have been reported when using Hele-Shaw cells with 100 μm cylindrical posts instead of packed beads[34]. By studying the capillary surface in a wedge, Concus and Finn[58] showed that a capillary surface is unstable if the relation $\theta + \alpha/2 \geq \pi/2$ is not satisfied, where θ are the contact and α the corner angle.

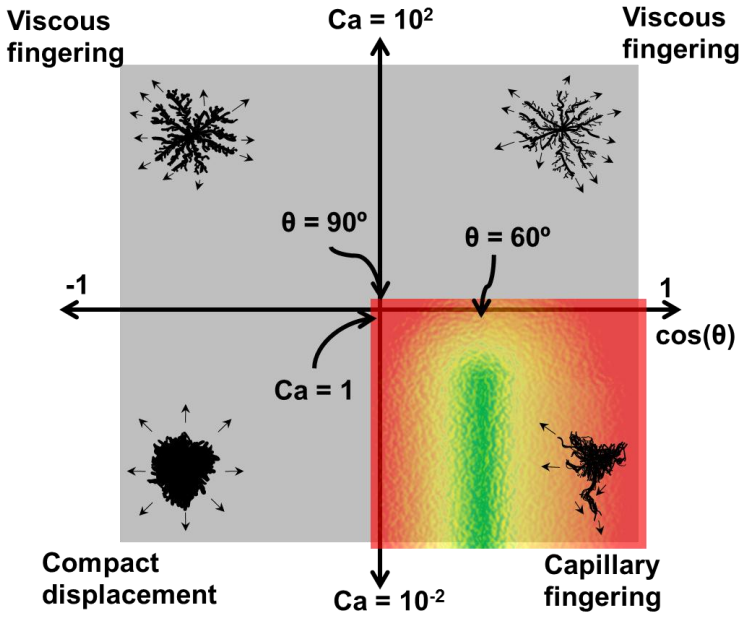

Figure 10. Fingering map where Ca is the ratio between viscous forces and capillary forces ($Ca = \mu_L u/\gamma$) and θ is the contact angle. Partially decreasing the global wettability of the particles can increase the mass transfer coefficient if viscous forces are controlled (e.g. lowering flow rates or increasing the reactor diameter).

One should bear in mind that trying wettability modification should be the result of a trade-off. Reducing the liquid affinity of the surface in a marked degree will result in a poorly wetted catalyst which can be more detrimental than channeling, e.g. due to the appearance of non-selective reactions and the occurrence of hotspots. The screening analysis performed and illustrated in Figures 7 and 8, identify the complex balance that the optimum contact-angle should achieve. The effect of contact angle in our simulations, supported by the experimental results mentioned above, can be sketched as in Figure 10. The green-shaded area indicates the region where the benefits of increasing the contact angle will be more significant —capillary fingering regimes. Reducing the gas-channeling via wettability control can lead to mass transfer

enhancements given the better radial distribution of the gas phase. If the interaction between the solvent and catalyst surface is designed to have an average contact angle of 60º, the aleatory nature of the packed-geometry may lead to hydrodynamic regimes where the fluid-fluid 'violent' invasions (or bursts) are continuously modified. This knowledge, supported by both our simulations and recent experimental results, demonstrate plenty of potential, especially when combined with the parameter tuning of the rest of operating conditions and design parameters.

A final comment should be devoted to discussing the significance of the values of contact angle for samples with a high degree of surface nonideality such as that of the particles in the packed bed. In the simulations presented above, a critical assumption is that the contact angle has a meaningful, definite value for the porous solid. In this respect, it has been shown that the contact angle can be measured in a straightforward way for packed beds composed of the typical substrates employed in heterogeneous catalysis, being the reported results in terms of surface interactions.[59]

Conclusions

In this work, we have dealt with the modeling and simulation of two-phase miniaturized packed-bed reactors. With the advances in new numerical methods and computational power, a physically-based model, named Phase Field Method (PFM), is applied to simulate two-phase flow in a microfabricated packed system found in the literature[10].

The main conclusions of this work are the following:

- The phase-field method (PFM) is able to simulate a two-phase flow micro-system reasonably well as compared to real experiments. Its physically oriented mathematical approach handles the complex pore geometries and the gas-liquid topological changes.

- PFM confirms how, upon reducing the particle size down to the order of a few micros, forces such as viscous stress and interfacial tension become significant, leading to gas preferential channels whose presence cannot be diminished by increasing flow rates.
- The proper control of surface contact angle can decrease significantly gas-channeling phenomena. Perhaps counter-intuitively, reducing the wettability of the particle surface to a certain extent (60 to 90º for capillary-driven flow regimes) leads to a flow regime where the gas-liquid-solid interaction is homogenously increased. The potential enhancement of gas-liquid interaction and reduction of gas channelling observed in our PFM simulations is backed by theory and supported by recent experimental studies in the literature.[24,31,33,34]

As for the next steps, we believe that miniaturized packed-bed reactors with intermediate wetting characteristics and small bed particles are worth to explore when mass-transfer is limited by gas-channeling phenomena. An immediate consequence will be the increase of reproducibility leading to more reliable flow maps and correlations. However, the proper choice of catalyst support and solvent or a surface treatment to modify the wetabbilty is not always possible. Silica and alumina supports are known for their high wettability (low contact angles) regardless of the nature of the solvent.[59] In those cases, hydroxyapatite materials interact with alcohols (e.g. ethanol or 1-propanol) allowing an intermediate wettability of the support Alternatively, the addition of fine materials that alter the average contact angle of the bed can be proposed as an unstructured gas flow distributors. For instance, adding PTFE microbeads into the bed will reduce the affinity of hidrophilic liquids, promoting gas-liquid interaction and reducing gas channeling issues. Clearly, this is still a challenging area of research. The reduction of

preferential channels at the wall, especially relevant when reactor diameter is increased (scale-up), is also within our scope for future research. We believe that the new ideas presented in this work, and the ensuing advances in both theoretical and experimental results, will likely have significant and practical impact on the design micropacked-bed reactors.

ACKNOWLEDGMENTS. This research was partially funded by the EU project MAPSYN: Microwave, Acoustic and Plasma SYNtheses, under grant agreement No. CP-IP 309376 of the European Union Seventh Framework Program.

Nomenclature

Symbol	SI Units	Description
$\boldsymbol{\mu}$	[Pa · s]	viscosity
$\boldsymbol{u}$	[m · s^{-1}]	velocity
$\boldsymbol{\gamma}$	[N · m^{-1}]	surface tension
$\mathbf{Ca}$	[-]	capillary number
$\boldsymbol{\theta}$	[rad]	contact angle
$\boldsymbol{F}$	[m^3 · s^{-1}]	volumetric flow rate
$\boldsymbol{D_f}$	[-]	fractal dimension
$\boldsymbol{\phi}$	[-]	order parameter
$\boldsymbol{C}$	[mol · m^{-3}]	concentration
$\boldsymbol{h}$	[-]	hold-up
$\boldsymbol{\alpha}$	[rad]	neighboring particle angle

Subscripts

Symbol	Description
L	Liquid phase
G	Gas phase

ASSOCIATED CONTENT

Supporting information

The Supporting Information is available free of charge on the ACS Publications website at DOI: 10.1021/acs.iecr.xxxxxxx.

Phase-field method: motivation, governing equations and boundary conditions. Fractal analysis to quantify the self-similarity of gas channeling patterns.

AUTHOR INFORMATION

Corresponding Author

*(Roberto Gómez) E-mail: roberto.gomez@ua.es

ORCID

Francisco J. Navarro-Brull: 0000-0001-7482-9485

Roberto Gómez: 0000-0002-5231-8032

NOTES

The authors declare no competing financial interest.

References

(1) Losey, M. W.; Schmidt, M. A.; Jensen, K. F. Microfabricated Multiphase Packed-Bed Reactors: Characterization of Mass Transfer and Reactions. *Ind. Eng. Chem. Res.* **2001**, *40*, 2555–2562.

(2) Losey, M. W.; Jackman, R. J.; Firebaugh, S. L.; Schmidt, M. A.; Member, S.; Jensen, K. F. Design and Fabrication of Microfluidic Devices for Multiphase Mixing and Reaction. *J. Microelectromech. Syst*. **2002**, *11*, 709–717.

(3) Losey, M. W.; Schmidt, M. A.; Jensen, K. F. A Micro Packed-Bed Reactor for Chemical Synthesis. In *Microreaction Technology: Industrial Prospects SE - 28*; Ehrfeld, W., Ed.; Springer Berlin Heidelberg, 2000; pp 277–286.

(4) Kolb, G.; Hessel, V. Micro-Structured Reactors for Gas Phase Reactions. *Chem. Eng. J.* **2004**, *98*, 1–38.

(5) Hessel, V.; Angeli, P.; Gavriilidis, A.; Löwe, H. Gas-Liquid and Gas-Liquid-Solid Microstructured Reactors: Contacting Principles and Applications. *Ind. Eng. Chem. Res.* **2005**, *44*, 9750–9769.

(6) Wegner, J.; Ceylan, S.; Kirschning, A. Ten Key Issues in Modern Flow Chemistry. *Chem. Commun.* **2011**, *47*, 4583–4592.

(7) Márquez, N.; Musterd, M.; Castaño, P.; Berger, R.; Moulijn, J. a.; Makkee, M.; Kreutzer, M. T. Volatile Tracer Dispersion in Multi-Phase Packed Beds. *Chem. Eng. Sci.* **2010**, *65*, 3972–3985.

(8) Zhang, J.; Teixeira, A. R.; Kögl, L. T.; Yang, L.; Jensen, K. F. Hydrodynamics of Gas-Liquid Flow in Micro-Packed Beds: Pressure Drop, Liquid Holdup and Two-Phase Model. *AIChE J.* **2017**, *63*, 1547-5905

(9) Wang, Y.; Chen, J.; Larachi, F. Modelling and Simulation of Trickle-Bed Reactors Using Computational Fluid Dynamics: A State-of-the-Art Review. *Can. J. Chem. Eng.* **2013**, *91*, 136–180.

(10) Marquez Luzardo, N. M. Hydrodynamics of Multi-Phase Packed Bed Micro-Reactors. *TU Delft* (Doctoral Thesis). **2010**. ISBN: 9789053352410.

(11) Horgue, P.; Augier, F.; Duru, P.; Prat, M.; Quintard, M. Experimental and Numerical Study of Two-Phase Flows in Arrays of Cylinders. *Chem. Eng. Sci.* **2013**, *102*, 335–345.

(12) Karadimitriou, N. K.; Musterd, M.; Kleingeld, P. J.; Kreutzer, M. T.; Hassanizadeh, S. M.; Joekar-Niasar, V. On the Fabrication of PDMS Micromodels by Rapid Prototyping, and Their Use in Two-Phase Flow Studies. *Water Resour. Res.* **2013**, *49*, 2056–2067.

(13) Saha, A. A.; Mitra, S. K.; Tweedie, M.; Roy, S.; McLaughlin, J. Experimental and Numerical Investigation of Capillary Flow in SU8 and PDMS Microchannels with Integrated Pillars. *Microfluid. Nanofluidics* **2009**, *7*, 451–465.

(14) van Herk, D.; Castaño, P.; Makkee, M.; Moulijn, J. A.; Kreutzer, M. T. Catalyst Testing in a Multiple-Parallel, Gas–liquid, Powder-Packed Bed Microreactor. *Appl. Catal. Gen.* **2009**, *365*, 199–206.

(15) Márquez, N.; Castaño, P.; Moulijn, J. A.; Makkee, M.; Kreutzer, M. T. Transient Behavior and Stability in Miniaturized Multiphase Packed Bed Reactors. *Ind. Eng. Chem. Res.* **2010**, *49*, 1033–1040.

(16) Alsolami, B. H.; Berger, R. J.; Makkee, M.; Moulijn, J. A. Catalyst Performance Testing in Multiphase Systems: Implications of Using Small Catalyst Particles in Hydrodesulfurization. *Ind. Eng. Chem. Res.* **2013**, *52*, 9069–9085.

(17) Moulijn, J. A.; Makkee, M.; Berger, R. J. Catalyst Testing in Multiphase Micro-Packed-Bed Reactors; Criterion for Radial Mass Transport. *Catal. Today* **2016**, *259*, 354–359.

(18) Powell, J. B. Application of Multiphase Reaction Engineering and Process Intensi Fi Cation to the Challenges of Sustainable Future Energy and Chemicals. *Chem. Eng. Sci.* **2016**, *157*, 15–25.

(19) Faridkhou, A.; Larachi, F. Two-Phase Flow Hydrodynamic Study in Micro-Packed Beds – Effect of Bed Geometry and Particle Size. *Chem. Eng. Process.* **2014**, *78*, 27–36.

(20) Faridkhou, A.; Hamidipour, M.; Larachi, F. Hydrodynamics of Gas–liquid Micro-Fixed Beds – Measurement Approaches and Technical Challenges. *Chem. Eng. J.* **2013**, *223*, 425–435.

(21) Olbricht, W. L. Pore-Scale Prototypes of Multiphase Flow in Porous Media. *Annu. Rev. Fluid Mech.* **1996**, *28*, 187–213.

(22) Faridkhou, A.; Tourvieille, J. N.; Larachi, F. Reactions, Hydrodynamics and Mass Transfer in Micro-Packed Beds Overview and New Mass Transfer Data. *Chem. Eng. Process. Process Intensif.* **2016**, *110*, 80–96.

(23) Trojer, M.; Szulczewski, M. L.; Juanes, R. Stabilizing Fluid – Fluid Displacements in Porous Media through Wettability Alteration. *Phys. Rev. Applied.* **2015**, *3*, 054008.

(24) Zhao, B.; MacMinn, C. W.; Juanes, R. Wettability Control on Multiphase Flow in Patterned Microfluidics. *Proc. Natl. Acad. Sci. U. S. A.* **2016**, *113*, 10251–10256.

(25) Holtzman, R. Effects of Pore-Scale Disorder on Fluid Displacement in Partially-Wettable Porous Media. *Sci. Rep.* **2016**, *6*, 36221

(26) Gong, H.; Li, Y.; Dong, M.; Ma, S.; Liu, W. Effect of Wettability Alteration on Enhanced Heavy Oil Recovery by Alkaline Flooding. *Colloids Surf. A.* **2016**, *488*, 28–35.

(27) Rabbani, H. S.; Joekar-Niasar, V.; Shokri, N. Effects of Intermediate Wettability on Entry Capillary Pressure in Angular Pores. *J. Colloid Interface Sci.* **2016**, *473*, 34–43.

(28) Hu, R.; Wan, J.; Kim, Y.; Tokunaga, T. K. Wettability Effects on Supercritical CO 2 – brine Immiscible Displacement during Drainage: Pore-Scale Observation and 3D Simulation. *Int. J. Greenh. Gas Con.* **2017**, *60*, 129–139.

(29) Herring, A. L.; Sheppard, A.; Andersson, L.; Wildenschild, D. Impact of Wettability Alteration on 3D Nonwetting Phase Trapping and Transport. *Int. J. Greenh. Gas Con.* **2016**, *46*, 175–186.

(30) Blunt, M. J. *Multiphase Flow in Permeable Media: A Pore-Scale Perspective*, 1st ed.; Cambrige University Press: University Printing House, Cambrige CB2 8BS, United Kingdom, 2017.

(31) Singh, K.; Scholl, H.; Brinkmann, M.; Michiel, M. Di; Scheel, M.; Herminghaus, S.; Seemann, R. The Role of Local Instabilities in Fluid Invasion into Permeable Media. *Sci. Rep.* **2017**, *7*, 444.

(32) Lenormand, R.; Touboul, E.; Zarcone, C. Numerical Models and Experiments on Immiscible Displacements in Porous Media. *J. Fluid Mech.* **1988**, *189*, 165–187.

(33) Trojer, M.; Szulczewski, M. L.; Juanes, R. Stabilizing Fluid-Fluid Displacements in Porous Media Through Wettability Alteration. *Phys. Rev. Appl.* **2015**, *3*, 1–8.

(34) Jung, M.; Brinkmann, M.; Seemann, R.; Hiller, T.; Herminghaus, S. Wettability Controls Slow Immiscible Displacement through Local Interfacial Instabilities. *Phys. Rev. Fluids* **2016**, *1*, 074202.

(35) Wörner, M. Numerical Modeling of Multiphase Flows in Microfluidics and Micro Process Engineering: A Review of Methods and Applications. *Microfluid. Nanofluidics* **2012**, *12*, 841–886.

(36) Akhlaghi Amiri, H. A.; Hamouda, A. A. Evaluation of Level Set and Phase Field Methods in Modeling Two Phase Flow with Viscosity Contrast through Dual-Permeability Porous Medium. *Int. J. Multiph. Flow.* **2013**, *52*, 22–34.

(37) Alpak, F. O.; Riviere, B.; Frank, F. A Phase-Field Method for the Direct Simulation of Two-Phase Flows in Pore-Scale Media Using a Non-Equilibrium Wetting Boundary Condition. *Comput. Geosci.* **2016**, *20*, 881-908.

(38) Akhlaghi Amiri, H. A.; Hamouda, A. A. Pore-Scale Modeling of Non-Isothermal Two Phase Flow in 2D Porous Media: Influences of Viscosity, Capillarity, Wettability and Heterogeneity. *Int. J. Multiph. Flow*. **2014**, *61*, 14–27.

(39) Ashish Saha, A.; Mitra, S. K. Effect of Dynamic Contact Angle in a Volume of Fluid (VOF) Model for a Microfluidic Capillary Flow. *J. Colloid Interface Sci.* **2009**, *339*, 461–480.

(40) Ferrari, A.; Jimenez-Martinez, J.; Le Borgne, T.; Mèheust, Y.; Lunati, I. Challenges Inmodeling Unstable Two-Phase Flow Experiments in Porousmicromodels. *Water Resour. Res.* **2015**, *51*, 1381–1400.

(41) Nieves-Remacha, M. J.; Yang, L.; Jensen, K. F. OpenFOAM Computational Fluid Dynamic Simulations of Two-Phase Flow and Mass Transfer in an Advanced-Flow Reactor. *Ind. Eng. Chem. Res.* **2015**, *54*, 6649–6659.

(42) Yang, L.; Shi, Y.; Abolhasani, M.; Jensen, K. F. Characterization and Modeling of Multiphase Flow in Structured Microreactors: A Post Microreactor Case Study. *Lab Chip* **2015**, *15*, 3232–3241.

(43) Harvie, D. J. E.; Davidson, M. R.; Rudman, M. An Analysis of Parasitic Current Generation in Volume of Fluid Simulations. *Appl. Math. Model.* **2006**, *30*, 1056–1066.

(44) Kunz, P.; Zarikos, I. M.; Karadimitriou, N. K.; Huber, M.; Nieken, U.; Hassanizadeh, S. M. Study of Multi-Phase Flow in Porous Media: Comparison of SPH Simulations with Micro-Model Experiments. *Transp. Porous Media* **2015**, *114*, 1–20.

(45) Tomin, P.; Lunati, I. Hybrid Multiscale Finite Volume Method for Two-Phase Flow in Porous Media. *J. Comput. Phys.* **2013**, *250*, 293–307.

(46) Tomin, P.; Lunati, I. Local–global Splitting for Spatiotemporal-Adaptive Multiscale Methods. *J. Comput. Phys.* **2015**, *280*, 214–231.

(47) Tomin, P.; Lunati, I. Investigating Darcy-Scale Assumptions by Means of a Multiphysics Algorithm. *Adv. Water Resour.* **2015**, *95*, 80-91.

(48) Tomin, P.; Lunati, I. Spatiotemporal Adaptive Multiphysics Simulations of Drainage-Imbibition Cycles. *Comput. Geosci.* **2016**, *20*, 541–554.

(49) Kim, J. Phase-Field Models for Multi-Component Fluid Flows. *Commun. Comput. Phys.* **2012**, *12*, 613–661.

(50) Kainourgiakis, M. E.; Kikkinides, E. S.; Stubos, A. K. Diffusion and Flow in Porous Domains Constructed Using Process-Based and Stochastic Techniques. *J. Porous Mater.* **2002**, *9*, 141–154.

(51) Atmakidis, T.; Kenig, E. Y. CFD-Based Analysis of the Wall Effect on the Pressure Drop in Packed Beds with Moderate Tube/Particle Diameter Ratios in the Laminar Flow Regime. *Chem. Eng. J.* **2009**, *155*, 404–410.

(52) Al-Rifai, N.; Galvanin, F.; Morad, M.; Cao, E.; Cattaneo, S.; Sankar, M.; Dua, V.; Hutchings, G.; Gavriilidis, A. Hydrodynamic Effects on Three Phase Micro-Packed Bed Reactor Performance - Gold-Palladium Catalysed Benzyl Alcohol Oxidation. *Chem. Eng. Sci.* **2016**, *149*, 129–142.

(53) Holtzman, R.; Segre, E. Wettability Stabilizes Fluid Invasion into Porous Media via Nonlocal, Cooperative Pore Filling. *Phys. Rev. Lett.* **2015**, *115*, 3–6.

(54) Xu, J.; Louge, M. Y. Statistical Mechanics of Unsaturated Porous Media. *Phys. Rev. E.* **2015**, *92*, 062405.

(55) Ashish Saha, A.; Mitra, S. K. Effect of Dynamic Contact Angle in a Volume of Fluid (VOF) Model for a Microfluidic Capillary Flow. *J. Colloid Interface Sci.* **2009**, *339*, 461–480.

(56) Singh, K.; Bijeljic, B.; Blunt, M. J. Imaging of Oil Layers, Curvature and Contact Angle in a Mixed-Wet and a Water-Wet Carbonate Rock. *Water Resour. Res.* **2016**, *52*, 1716–1728.

(57) Singh, K.; Scholl, H.; Brinkmann, M.; Michiel, M. D.; Scheel, M.; Herminghaus, S.; Seemann, R. The Role of Local Instabilities in Fluid Invasion into Permeable Media. *Sci. Rep.* **2017**, *7*, 444.

(58) Finn, R. On the Behavior of a Capillary Surface at a Singular Point. *J. Analyse Math.* **1976**, *30*, 156–163.

(59) Jaine, J. E.; Mucalo, M. R. Measurements of the Wettability of Catalyst Support Materials Using the Washburn Capillary Rise Technique. *Powder Technol.* **2015**, *276*, 123–128.

TOC/Abstract graphic